Kinetic isotope effects on thio-substituted biological phosphoryl transfer reactions from density-functional theory

Yun Liu,[a] Xabier Lopez[b] and Darrin M. York*[a]

Received (in Cambridge, MA, USA) 22nd February 2005, Accepted 23rd May 2005
First published as an Advance Article on the web 6th July 2005
DOI: 10.1039/b502568k

Primary and secondary kinetic and equilibrium isotope effects are calculated with density-functional methods for the dianionic methanolysis of the native (unsubstituted) and thio-substituted ethylene phosphates.

The study of the non-enzymatic and enzymatic mechanisms of phosphoryl transfer reactions has a rich history both with experimental and theoretical methods.[1–4] Nonetheless, the mechanistic details of many important biological phosphoryl transfer processes remain elusive. A powerful experimental approach to characterize transition states in phosphoryl transfer reactions involves the measurement of isotope effects.[4,5] A change in reaction rate constant or equilibrium constant that results from isotope substitution is known as a kinetic or equilibrium isotope effect (KIE or EIE). KIE and EIE measurements are sensitive probes for specific changes in bonding, and have been applied to study both enzymatic and non-enzymatic reactions.[6] Further insight into mechanism can be gained by the introduction of site-specific chemical modifications, such as thio-substitution at the key phosphoryl oxygen positions.[7] A resulting change in the reaction rate is termed a "thio effect".[3,7] The study of kinetic isotope effects for a series of thio-substituted phosphoryl transfer reactions offers two-fold insight into the nature of the transition states and reaction mechanisms.

Theoretical methods have considerable promise in the elucidation of important details of biological phosphoryl transfer reactions,[8–11] and may assist in the mechanistic interpretation of experimental data.[12,13] However, experimental data are crucial to validate existing theoretical methods and influence the design of new-generation models. The study of phosphoryl transfer reactions[14–16] that involve highly charged intermediates and interaction with solvent and metal ions is particularly challenging.

In the present work, density-functional methods are used to study primary and secondary kinetic and equilibrium isotope effects[4,6] on the dianionic reaction mechanism for methanolysis of ethylene phosphate (Scheme 1), a reverse reaction model for RNA phosphate transesterification under alkaline conditions.[1] In addition, a series of five thio-substitutions[16,17] at the key phosphoryl oxygen positions are considered. Two primary and three secondary (^{18}O and ^{34}S) isotope effects are considered for each of the in-line dianionic reactions: the native (unsubstituted) reaction, singly-substituted reactions at the non-bridging O_{P1} position and bridging $O_{2'}$, $O_{3'}$ and $O_{5'}$ positions, and a doubly-substituted reaction at the O_{P1} and O_{P2} positions.

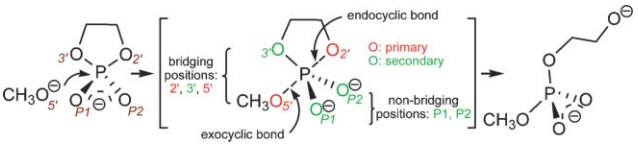

Scheme 1 Kinetic isotope effects in the in-line dianionic mechanism of ethylene phosphate methanolysis (a reverse-reaction model for RNA phosphate transesterification). The numbering scheme corresponds to that of the RNA system.

Density-functional calculations were performed using the B3LYP exchange-correlation functional[18,19] with the 6-31++G(d,p) basis set for geometry and frequency calculations followed by single-point energy refinement and natural bond order (NBO) analysis[20] with the 6-311++G(3df,2p) basis set in a manner analogous to recent studies of biological phosphates.[21–24] Solvent was treated using the PCM solvation model,[25,26] with UAKS radii.[27] All calculations are performed with the GAUSSIAN03.[28] Solvation effects were based on gas phase-optimized geometries as in prior work.[21–24]

A comparison of thermodynamic quantities for the rate-controlling transition states is given in Table 1. All the reactions in the present work correspond to associative or concerted mechanisms.[13] The gas-phase reaction barriers are large due to the association of monoanionic reactants to form a dianionic transition state. Solvation has a tremendous transition state stabilization effect, with $\Delta\Delta G_{sol}$ values ranging from −45.6 to −57.2 kcal/mol. In aqueous solution, the native reaction has an activation free energy barrier of 41.1 kcal/mol and reaction free energy of 12.8 kcal/mol, and is characterized by an early transition state with a large P–$O_{5'}$ bond length (2.453 Å, Table 2) and low bond order (0.210, Table 3), large accumulation of charge on the 5′ oxygen (−0.911 *e*, Table 4), and an almost fully formed leaving group P–$O_{2'}$ bond. Single and double sulfur substitutions at the non-bridging positions lead to a decrease in the associative

Table 1 Comparison of thermodynamic quantities (kcal/mol) for the rate-controlling transition states for dianionic transphosphorylation

Reaction	ΔE	ΔH	$-T\Delta S$	ΔG	$\Delta\Delta G_{sol}$	ΔG_{aq}
native	87.2	87.1	11.2	98.3	−57.2	41.1
S:O_{P1}	82.4	82.5	10.5	93.0	−52.4	40.6
S:O_{P1}, O_{P2}	79.6	79.8	10.5	90.3	−48.7	41.6
S:$O_{3'}$	77.3	77.8	11.6	89.4	−53.1	36.3
S:$O_{5'}$	99.4	98.0	10.1	108.0	−52.1	55.9
S:$O_{2'}$	78.5	78.8	9.2	88.0	−45.6	42.4

[a]*Department of Chemistry, University of Minnesota, 207 Pleasant St. SE, Minneapolis, MN 55455, USA. E-mail: york@chem.umn.edu; Fax: 612 626 2006; Tel: 612 624 8042*
[b]*Kimika Fakultatea, Euskal Herriko Unibertsitatea, P.K. 1072, 20080, Donostia, Euskadi, Spain*

Table 2 P–X bond lengths r (Å) in the rate-controlling transition state

Reaction	$r_{X5'}$	$r_{X2'}$	$r_{X3'}$	r_{XP1}	r_{XP2}
native	2.453	1.841	1.723	1.506	1.514
S:O_{P1}	2.655	1.781	1.706	2.031	1.502
S:O_{P1}, O_{P2}	2.823	1.767	1.701	2.011	2.005
S:$O_{3'}$	2.329	1.815	2.247	1.520	1.511
S:$O_{5'}$	2.537	2.513	1.664	1.500	1.501
S:$O_{2'}$	2.757	2.538	1.655	1.493	1.500

Table 3 P–X bond orders BO in the rate-controlling transition state[a]

Reaction	$BO_{X5'}$	$BO_{X2'}$	$BO_{X3'}$	BO_{XP1}	BO_{XP2}
native	0.210	0.648	0.817	1.679	1.646
S:O_{P1}	0.172	0.726	0.845	1.550	1.707
S:O_{P1}, O_{P2}	0.154	0.737	0.832	1.628	1.649
S:$O_{3'}$	0.265	0.675	0.827	1.594	1.639
S:$O_{5'}$	0.527	0.188	0.912	1.684	1.689
S:$O_{2'}$	0.124	0.491	0.912	1.759	1.714

[a] Shown are the NBO[20] P–X normalized bond orders. The P–O bond orders were normalized by a scale factor of 1.423, defined such that the native reaction has a sum of P–O bond orders equal to 5.0. This scale factor was applied to all P–O bond orders in the thio-substituted reactions. The P–S bond orders were scaled such that the sum of the normalized P–O and P–S bond orders was equal to 5.0.

Table 4 NBO charge values Q (*au*) for the key phosphoryl oxygens (sulfurs) and phosphorus in the rate-controlling transition states[a]

Reaction	$Q_{5'}$	$Q_{2'}$	$Q_{3'}$	Q_{P1}	Q_{P2}	Q_P
native	−0.911	−0.863	−0.835	−1.165	−1.182	2.507
S:O_{P1}	−0.905	−0.860	−0.837	−0.832	−1.133	2.081
S:O_{P1}, O_{P2}	−0.896	−0.862	−0.839	−0.729	−0.715	1.539
S:$O_{3'}$	−0.903	−0.866	−0.192	−1.188	−1.167	2.233
S:$O_{5'}$	−0.441	−0.873	−0.868	−1.149	−1.146	2.385
S:$O_{2'}$	−0.925	−0.447	−0.846	−1.118	−1.135	2.386

[a] Shown are the NBO[20] charge values (Q_X) in *au*, where X indicates either an oxygen or sulfur atom bonded to P, or the P center itself.

character of the transition state (in terms of P–$O_{5'}$ bond lengths and bond orders).

Sulfur substitution at the non-bridging positions lowers the activation barrier in the gas phase due to an electronic stabilization effect of the softer ligands on the dianionic transition state. However, the larger sulfur atoms are less well solvated than the oxygens, and this reduced stabilization tends to cancel the favorable electronic effect in the gas phase such that the activation barrier in solution is only mildly affected by sulfur substitution. These results are qualitatively consistent with experimental data for RNA analogs with non-bridging thio substitutions that exhibit only modest thio effects.[3,29,30]

Substitution at the bridging $O_{3'}$ position leads to an increase in associative character of the transition state that is accompanied by a lowering of the activation barrier by 4.8 kcal/mol. This is consistent with the experimentally observed 200-fold[31] and 2000-fold[32] rate enhancements observed for 3′-thio modified RNA dinucleotides. Thio substitution at the $O_{2'}$ position leads to a transition state with the least associative character ($r_{X5'}$ = 2.757 Å, $BO_{X5'}$ = 0.124) and considerable decrease in the reaction free energy (−8.8 kcal/mol). This considerably raises the barrier of the reverse reaction and is consistent with kinetic measurements for

Table 5 Primary and secondary KIE and EIE values for thio-substituted dianionic transphosphorylation reactions[a]

	Primary		Secondary		
Reaction	$X_{5'}$	$X_{2'}$	$X_{3'}$	X_{P1}	X_{P2}
Kinetic Isotope Effects (KIEs)					
native	1.0214	1.0064	1.0032	0.9947	0.9958
S:O_{P1}	1.0258	1.0042	1.0074	1.0021	1.0042
S:O_{P1}, O_{P2}	1.0258	1.0053	1.0032	1.0011	1.0021
S:$O_{3'}$	1.0171	1.0107	1.0032	1.0021	1.0053
S:$O_{5'}$	0.9990	1.0466	0.9990	0.9958	0.9958
S:$O_{2'}$	1.0149	1.0032	1.0011	1.0011	1.0000
Equilibrium Isotope Effects (EIEs)					
native	0.9636	1.0334	0.9979	0.9937	0.9937
S:O_{P1}	0.9626	1.0367	1.0000	1.0011	1.0032
S:O_{P1}, O_{P2}	0.9646	1.0301	1.0000	1.0011	1.0011
S:$O_{3'}$	0.9646	1.0323	1.0000	1.0032	1.0021
S:$O_{5'}$	0.9937	1.0345	0.9989	0.9947	0.9958
S:$O_{2'}$	0.9646	1.0064	1.0000	1.0011	1.0000

[a] A KIE value is defined as k/k' where k and k' are the rate constants for the light and heavy isotopes, respectively. EIE values are similarly defined using the corresponding equilibrium constants. Isotope substitutions include ^{18}O for oxygen and ^{34}S for sulfur, and are calculated at 298.15 K within the quantum harmonic oscillator approximation, neglecting tunnelling effects and changes in the transmission coefficient.

modified 2′-thio ribonucleotides that indicate thiolate attack to the phosphate center is 10^7 times slower than that of the corresponding alkoxide. Thio substitution at the $O_{5'}$ position results in the largest activation barrier and reaction free energy. This is largely due to the increased stability of the thiolate nucleophile (methanethiol has a pK_a value 5 units lower than methanol[33]).

The predicted KIE and EIE values for the native and thio-substituted reactions are listed in Table 5. KIE values in the present work were calculated from the full vibrational and rotational partition functions within the harmonic oscillator/rigid rotor approximations, as implemented in GAUSSIAN03.[28] The primary KIEs are most prominent at the 5′ position for all the reactions with the exception of the 5′ thio substitution (S:$O_{5'}$). KIE measurements have been made for the cyclization of uridine 3′-*m*-nitrobenzyl phosphate at different pH values,[34] the reverse reaction for which is analogous to that of the present work. A normal primary KIE (1.027) was measured under basic conditions (pH 10.5) that was interpreted as evidence of a concerted mechanism with the departure of an almost fully charged leaving group.[34] The calculated primary KIE value at the 5′ position for the native reaction (1.0214), along with the data in Tables 2–4, is consistent with the experimental results and interpretation.

With the exception of the S:$O_{5'}$ reaction, the KIE values for ^{18}O substitution at the 5′ position are normal (greater than unity) and correlated with the occurrence of an early $TS_{5'}$-type rate-controlling transition state characterized by an elongated P–$O_{5'}$ bond with low bond order and accumulation of charge at the 5′ nucleophilic oxygen. The normal primary KIE values at the 5′ position are due, in part, to a decrease in the $C_{5'}$–$O_{5'}$ bond order that occurs in going from reactant to the TS. The 5′ thio substitution reaction (S:$O_{5'}$) exhibits a prominent normal primary KIE at the 2′ position for ^{18}O substitution (1.0466), whereas an inverse KIE (0.9990) is observed for ^{34}S substitution at the 5′ position. The rate-controlling transition state for this reaction is shifted to that of a late $TS_{2'}$-type with significant accumulated

P–$S_{5'}$ bonding and increased associative character with respect to the nucleophile. As has been noted by others,[12,13] although measurements of isotope effects provide valuable information about mechanism, they may not decisively distinguish between associative and dissociative pathways. These results underscore the importance of continued evaluation and improvement of theoretical methods that may aid in the interpretation of experiments, and provide deeper insight into the mechanism of biological phosphoryl transfer processes.

The native and 5′ thio substitution reactions show inverse (less than 1) secondary KIE values at the non-bridging positions in contrast to the corresponding normal KIE values for the other reactions. This suggests that these transition states have considerable metaphosphate-like character[4] (*i.e.*, increased non-bridging P–X_{P1}/X_{P2} bond orders), and is consistent with the lengthening of the P–$O_{2'}$ bonds in the rate-controlling transition state. However, an alternative measure of metaphosphate character involves the sum of the bond orders of the phosphorus bonds to the nucleophilic and leaving group positions. Based on this index, the data in Table 3 would suggest that the thio-substituted S:$O_{2'}$ and S:$O_{5'}$ reactions have the most metaphosphate-like character. It should be pointed out that the numerical values of the bond orders in Table 3, despite the normalization procedure that was employed, are somewhat subjective, especially when comparing different types of bonds. Although for phosphate monoester systems inverse secondary KIE values and other measures of metaphosphate-like character have been interpreted as indicative of a dissociative mechanism, for the cyclic phosphate diester systems of the present work, these characteristics are consistent with concerted and associative mechanisms.

It is noteworthy that the inverse non-bridging KIE (X_{P2}) in the native reaction (0.9958) changes to normal (1.0042) upon sulfur substitution at the other non-bridging position (S:O_{P1}), even though these reactions bear fairly close overall resemblance (Table 1). This is intriguing in that a similar change was observed from an inverse non-bridging ^{18}O KIE in the hydrolysis of the *p*-nitrophenyl phosphate dianion to a normal non-bridging ^{18}O KIE for *p*-nitrophenyl phosphorothioate hydrolysis,[35] despite the similarity of these reactions as indicated by other measurements.[36] The primary and secondary KIEs for the 3′-thio substituted reaction suggest that this transition state is tighter and more phosphorane-like than that of the native reaction.

The primary EIEs are all normal (greater than 1) for isotope substitution at the 2′ position and inverse for substitution at the 5′ position. This indicates a preference for the heavier isotope to occupy a tighter bonding arrangement. The 5′ ^{18}O or ^{34}S isotopes proceed from a more stiff bond with carbon in the reactant alkoxide/thiolate to a more loose bonding arrangement in the phosphate/phosphorothioate product. The situation is reversed when these isotopes occupy the 2′ position. The secondary EIEs are small and normal with the exception of the native and 5′ thio-substituted reactions, suggesting a slight loosening occurs in going to the product state.

Taken together, these results provide insight into the nature of isotope effects in phosphoryl transfer reactions with thio substitutions important for the mechanistic characterization of enzymes and ribozymes. It is the hope that further integration of theory and experiment may lead to the design of new-generation quantum methods capable of modeling phosphoryl transfer reactions with improved accuracy and reliability.

DY is grateful for financial support provided by the National Institutes of Health (Grant 1R01-GM62248-01A1), and thanks Francesca Guerra and Alvan Hengge for insightful comments on the manuscript. Computational resources were provided by the Minnesota Supercomputing Institute.

Notes and references

1 D. Perreault and E. Anslyn, *Angew. Chem. Int. Ed.*, 1997, **36**, 432.
2 D. Zhou and K. Taira, *Chem. Rev.*, 1998, **98**, 991.
3 M. Oivanen, S. Kuusela and H. Lönnberg, *Chem. Rev.*, 1998, **98**, 961.
4 A. Hengge, *Acc. Chem. Res.*, 2002, **35**, 105.
5 J. Marlier, *Acc. Chem. Res.*, 2001, **34**, 283.
6 A. Hengge, *FEBS Lett.*, 2001, **501**, 99.
7 D. Herschlag, J. Piccirilli and T. Cech, *Biochemistry*, 1991, **30**, 4844.
8 A. Warshel, *Computer Modeling of Chemical Reactions in Enzymes and Solutions*; John Wiley and Sons: New York, 1991.
9 M. Karplus, *J. Phys. Chem. B*, 2000, **104**, 11.
10 A. Warshel, *Annu. Rev. Biophys. Biomol. Struct.*, 2003, **32**, 425.
11 M. Garcia-Viloca, J. Gao, M. Karplus and D. Truhlar, *Science*, 2004, **303**, 186.
12 J. Florián, J. Åqvist and A. Warshel, *J. Am. Chem. Soc.*, 1998, **120**, 11524.
13 J. Åqvist, K. Kolmodin, J. Florián and A. Warshel, *Chem. Biol.*, 1999, **6**, R71.
14 J. Florián and A. Warshel, *J. Phys. Chem. B*, 1998, **102**, 719.
15 C. Hu and T. Brinck, *J. Phys. Chem. A*, 1999, **103**, 5379.
16 B. Gregersen, X. Lopez and D. York, *J. Am. Chem. Soc.*, 2004, **126**, 7504.
17 B. Gregersen, X. Lopez and D. York, *J. Am. Chem. Soc.*, 2003, **125**, 7178.
18 C. Lee, W. Yang and R. Parr, *Phys. Rev. B*, 1988, **37**, 785.
19 A. Becke, *J. Chem. Phys.*, 1993, **98**, 5648.
20 A. Reed, R. Weinstock and F. Weinhold, *J. Chem. Phys.*, 1985, **83**, 735.
21 K. Range, M. McGrath, X. Lopez and D. York, *J. Am. Chem. Soc.*, 2004, **126**, 1654.
22 E. Mayaan, K. Range and D. York, *J. Biol. Inorg. Chem.*, 2004, **9**, 807.
23 C. López, O. Faza, A. de Lera and D. York, *Chem. Eur. J.*, 2005, **11**, 2081.
24 C. López, O. Faza, B. Gregersen, X. Lopez, A. de Lera and D. York, *Chem. Phys. Chem.*, 2004, **5**, 1045.
25 J. Tomasi and M. Persico, *Chem. Rev.*, 1994, **94**, 2027.
26 M. Cossi, G. Scalmani, N. Rega and V. Barone, *J. Chem. Phys.*, 2002, **117**, 43.
27 V. Barone, M. Cossi and J. Tomasi, *J. Chem. Phys.*, 1997, **107**, 3210.
28 M. Frisch, *Gaussian 03, Revision B.01*, Gaussian, Inc., Pittsburgh, PA, 2003.
29 H. Almer and R. Strömberg, *Tetrahedron Lett.*, 1991, **32**, 3723.
30 M. Ora, J. Järvi, M. Oivanen and H. Lönnberg, *J. Org. Chem.*, 2000, **65**, 2651.
31 X. Liu and C. Reese, *Tetrahedron Lett.*, 1996, **37**, 925.
32 L. Weinstein, D. Earnshaw, R. Cosstick and T. Cech, *J. Am. Chem. Soc.*, 1996, **118**, 10341.
33 D. Lide, Ed.; *CRC handbook of chemistry and physics*; CRC Press LLC: Boca Raton, FL, 83rd edn.; 2003.
34 B. Gerratana, G. Sowa and W. Cleland, *J. Am. Chem. Soc.*, 2000, **122**, 12615.
35 I. Catrina and A. Hengge, *J. Am. Chem. Soc.*, 2003, **125**, 7546.
36 I. Catrina and A. Hengge, *J. Am. Chem. Soc.*, 1999, **121**, 2156.